Genes & Diseases (2022) 9, 1315–1331

Available online at www.sciencedirect.com

ScienceDirect

journal homepage: http://ees.elsevier.com/gendis/default.asp

FULL LENGTH ARTICLE

Estrogen deficiency exacerbates learning and memory deficits associated with glucose metabolism disorder in APP/PS1 double transgenic female mice

Min Luo [a,b,1], Qinghua Zeng [a,c,1], Kai Jiang [d], Yueyang Zhao [a], Zhimin Long [a,c], Yexiang Du [a], Kejian Wang [a,c,*], Guiqiong He [a,c,]**

[a] *Chongqing Key Laboratory of Neurobiology, Chongqing Medical University, Chongqing 400016, PR China*
[b] *Department of Pathology, Suining Municipal Hospital of TCM, Suining, Sichuan 629000, PR China*
[c] *Department of Anatomy, Chongqing Medical University, Chongqing 400016, PR China*
[d] *Department of Gastroenterology, Suining Central Hospital, Suining, Sichuan 629000, PR China*

Received 28 October 2020; received in revised form 15 January 2021; accepted 27 January 2021
Available online 16 February 2021

KEYWORDS
Alzheimer's disease;
Estrogen deficiency;
Glucose metabolism disorder;
GSK-3β;
IGF-1;
Mitochondria

Abstract Alterations in glucose metabolism occur in the brain in the early stage of Alzheimer's disease (AD), and menopausal women have more severe metabolic dysfunction and are more prone to dementia than men. Although estrogen deficiency-induced changes in glucose metabolism have been previously studied in animal models, their molecular mechanisms in AD remain elusive. To investigate this issue, double transgenic (APP/PS1) female mice were subjected to bilateral ovariectomy at 3 months of age and were sacrificed 1 week, 1 month and 3 months after surgery to simulate early, middle and late postmenopause, respectively. Our analysis demonstrated that estrogen deficiency exacerbates learning and memory deficits in this mouse model of postmenopause. Estrogen deficiency impairs the function of

* Chongqing Key Laboratory of Neurobiology, Chongqing Medical University, Chongqing 400016, PR China.
** Corresponding author. Chongqing Key Laboratory of Neurobiology, Chongqing Medical University, No. 1 YiXueYuan Road, YuZhong District, Chongqing 400016, PR China. Fax: +86 023 89129930.
E-mail addresses: wangkejian@cqmu.edu.cn (K. Wang), guiqionghe@cqmu.edu.cn (G. He).
Peer review under responsibility of Chongqing Medical University.
[1] These authors have contributed equally to this work.

https://doi.org/10.1016/j.gendis.2021.01.007

mitochondria in glucose metabolism. It is possible that the occurrence of AD is associated with the aberrant mitochondrial ERβ-mediated IGF-1/IGF-1R/GSK-3β signaling pathway. In this study, we established a potential mechanism for the increased risk of AD in postmenopausal women and proposed a therapeutic target for AD due to postmenopause.

Introduction

Alzheimer's disease (AD), also known as dementia, is a neurodegenerative disease that is highly associated with age and causes the gradual loss of memory and cognitive function.[1] As aging progresses, the cumulative risk of AD increases. According to demographic information, it has been predicted that the worldwide population of individuals with AD will exceed 100 million by 2050.[2] This will undoubtedly place substantial economic and mental burdens on patients, their families, and society. The main pathological features of AD include senile plaques (SPs) formed by extracellular amyloid β peptide (Aβ) deposition, neurofibrillary tangles (NFTs) formed by intracellular tau hyperphosphorylation, synaptic reduction in the hippocampus and cortex, and degeneration and loss of neurons caused by lesions.[3] Currently, the etiology and pathogenesis of AD are still unclear, and no effective therapeutic strategy has been reported to prevent and delay the progression of AD.

A large number of epidemiological surveys have shown that the incidence of AD in postmenopausal women is approximately three times higher than that in men of the same age.[4,5] A decline in estrogen level is closely related to the high risk of AD in women during different menopausal stages. Usually, endogenous estrogen deficiency occurs before the onset of AD.[6] Estrogen can promote the growth and survival of memory-associated cholinergic neurons, inhibit the production and toxicity of Aβ, ameliorate neurotrophy, and reduce the hyperphosphorylation of tau protein.[7] Estrogen also plays a key role in the central regulation of energy homeostasis.[8] Estrogen exerts biological effects through its receptors. ERα acts as a transcription factor in the reproductive system and during human development, and ERβ is widely expressed in the cortex, hippocampus and other brain areas associated with learning and memory.[9,10] In recent years, many studies have confirmed the presence of estrogen receptors in mitochondria, and further studies have shown that ERβ in the brain is mainly localized to mitochondria.[11–13]

With the rapid development of neuroimaging technology, PET has become a reliable tool for the diagnosis of AD.[14] Many studies have shown that a decreased cerebral glucose metabolic rate is one of the common changes in AD. Energy metabolism in the brain has been shown to decrease before the appearance of clinical symptoms and cortical atrophy.[15,16] Furthermore, clinical studies have shown that severe metabolic disorders occur in the brains of postmenopausal women, and age-related decreases in metabolism are more prominent in women than in men.[17] Insulin-like growth factor-1 (IGF-1) is a potent trophic factor that binds its cognate receptor as a ligand and plays an important role in the energy metabolism of nerve cells, and the levels of IGF-1 substantially decline with age.[18,19] IGF-1 and the dimerization and trans-autophosphorylation of the intracellular kinase domains of its cognate receptor activate downstream signaling cascades, including the prototypical PI3K/AKT pathway, which drives cell survival and growth, and the glycogen synthase kinase-3β (GSK-3β) pathway, which is closely related to the three characteristic pathological changes of AD.[20,21] However, the molecular mechanism of IGF-1 in AD is still unclear.

In this study, we showed that spatial learning and memory deficits as well as a large amount of neuritic plaque deposition were associated with long-term estrogen deficiency. More importantly, ovariectomy (OVX) induced impairments in mitochondrial energy metabolism. To elucidate the potential mechanism by which estrogen deficiency exacerbates energy metabolism and cognitive dysfunction, the aberrant mt-Erβ-mediated downregulation of the IGF-1/IGF-1R/GSK-3β signaling pathway was investigated.

Materials and methods

Animals

Three-month-old APP/PS1 double transgenic female mice expressing a chimeric mouse/human amyloid precursor protein (Mo/Hu APP695swe) and a presenilin 1 delta exon 9 mutation (PS1-dE9) ([D000268] B6/JNju-Tg (APPswe, PSEN1dE9)/Nju) were purchased from the Nanjing Biomedical Research Institute of Nanjing University (Approval Number: SCXK (Su) 2015-0001). Mice were housed in groups of five in the IVC transgenic room of Chongqing Medical University Animal Center under a 12 h light/12 h dark cycle at constant temperature with food and water provided ad libitum. The animal procedures conformed to

Table 1 Basic information of clinical human brain tissue.

Group	Case	Age	Sex	Cause of death
Aged	1	97	M	Multiple organ failure
	2	88	M	Coronary heart disease
	3	87	M	brain tumor
	4	70	F	septicemia
AD	1	99	F	AD, cerebral stroke
	2	88	M	AD
	3	82	M	AD
	4	70	M	AD

the guidelines of the Ethics Committee of Chongqing Medical University.

Postmortem human brains

We obtained human brain tissue from the human brain bank of Xiangya Medical College of South Central University. Samples from clinically diagnosed AD patients and age-matched non-AD subjects were selected for use in the present study (Table 1). Neuropathological changes in AD brains were evaluated using Braak's staging system, and cases with a clinical history of dementia and a Braak's stage of IV or higher were selected for study. The cases in the control group showed no or only mild amyloid and/or tau pathology in the cerebrum, and neuropathology was limited to Braak's stages I–II. All human brains were preserved according to a standardized procedure with one side of each brain rapidly frozen and stored at −70 °C for future biochemical studies and the other side immersion fixed in 10% formalin for anatomical/pathological studies. In the present study, sections from a slice of the mid-hippocampal temporal lobe (~2 cm thick) were used. The temporal lobe block was removed from the formalin-fixed hemisphere, cryoprotected in 30% sucrose, and cut at the frontal plane using a cryostat into 12 sets of sections (40 μm thick), with each set consisting of four equally sized (12 x 40 μm or ~500 μm^2) sections. The sections were then stored in a cryoprotectant at −20 °C until histological processing.

Experimental design and ovariectomy

Three-month-old female AD model mice and their littermates were randomly divided into two groups: the bilateral ovariectomized (AD-OVX) group and the sham operation group (AD-Sham) ($n = 18$). Wild-type mice (WT-OVX, WT-Sham) of the same age were selected as controls. Mice were anesthetized with 0.1% pentobarbital. After skin disinfection, a skin incision approximately 0.5 cm in length was made along the posterior midline of the back on the level of the connecting line between the bilateral upper margin of the hindlimb root. White fat masses close to the lower pole of the kidney, which are important anatomical landmarks for locating the ovary, were viewed through the thin muscle layer. After bilateral ovariectomy, the incisions were sutured. The sham operation groups underwent a similar procedure except that the ovaries were not removed. The mice were evaluated 1 week, 1 month, and 3 months after surgery.

Morris water maze

The Morris water maze was used to examine spatial learning and memory. The maze consisted of a circular pool approximately 1 m in diameter. The pool was divided into 4 quadrants with an escape platform approximately 10 cm in diameter placed in one quadrant. The water temperature was maintained at approximately 25 °C.

The experiment consisted of a place navigation test and a spatial probe test. The place navigation test lasted for six days. On the first day, a visible platform experiment was performed: the platform was exposed 1 cm above the water so that the mice could easily find it. The mice were placed in the water according to the established procedure, and the movement of the mice during the experiment was recorded by an image tracking system; the time to find the platform within a 60-s escape latency and the path length were measured. If a mouse did not find the platform at the end of the 60-s period, the experimental operators guided the mouse to the platform and allowed the mouse to remain on the platform for 15 s to learn its location. For the next three days, hidden platform experiments were performed: the platform position was fixed during the entire process, and the mice were placed in the water at different locations. The training method was the same as that in the visible platform experiment. On the seventh day, the spatial probe test was performed: the platform was removed, and the mice were allowed to swim freely in the pool for 1 min. The number of times each mouse passed across the platform was recorded on the probe day.

Tissue preparation and mitochondrial extraction

The experimental animals were deeply anesthetized and transcardially perfused with ice-cold 0.9% saline solution. Following perfusion, half of the brain extracted from the skull was stored at −80 °C and prepared for protein and mitochondrial analysis. The other half of the brain was postfixed in freshly prepared 4% paraformaldehyde (PFA) overnight at 4 °C and then dehydrated in a gradient of 20% and 30% sucrose and 0.1 M phosphate-buffered saline (PBS, pH = 7.4) until it sank and embedded in tissue embedding medium (4583, OCT Compound; Sakura Finetek Tissue-Tek, Tokyo, Japan). Coronal sections (10 μm thick) encompassing the entire cortex and hippocampus were cut with a freezing microtome (CM1860; Leica, Wetzlar, Germany), collected sequentially in 6-well plates filled with 0.01 M PBS and mounted onto slides for immunofluorescence analysis. Uteri were dissected and weighed. The manufacturer's instructions for the mitochondrial extraction kit (SM0020, Beijing Solarbio Science & Technology Co., Ltd.) were followed closely. We obtained high purity mitochondria by the differential centrifugation method. It is worth noting that all of the abovementioned procedures should be performed at a low temperature.

Immunohistochemistry analysis

Brain tissue sections were immunohistochemically stained with a specific kit (SA1020; Boster Bio, Wuhan, China). The sections were immunostained with biotin anti-β-amyloid 17–24, monoclonal 4G8 antibody (1:250, #800704; BioLegend, San Diego, CA, USA) and an anti-MAP2 antibody (1:1000, #4542, Abcam, Cambridge, USA) overnight at 4 °C. The next day, the sections were washed with 0.01 M PBS

three times for five minutes each. Then, the sections were incubated with secondary antibody for 30 min at 37 °C, and the plaques were stained with a DAB Kit (ZLI-9018, 1:20 mixture of solutions 1 and 2; ZSGB-BIO, Beijing, China). After another three washes with PBS, the sections were covered with coverslips, and images were captured on a Leica DM 4000 digital microscope (Leica, Wetzlar, Germany).

Transmission electron microscopy

Cardiac perfusion with a preprepared solution (a mixture of glutaraldehyde and paraformaldehyde) was performed after anesthesia. After perfusion, the brain was quickly removed and separated from the hippocampus, and approximately 1 mm^3 of tissue was removed with a scalpel. The sample was immediately fixed in a preprepared stationary solution (containing 3% glutaraldehyde, 1.5% paraformaldehyde, and 0.1 M PBS, pH = 7.2). Then, the following steps were performed: osmotic acid fixation; buffer flushing; dehydration in gradient alcohol and acetone; entrapment after penetration of entrapment agent; polymerization at 36 °C—60 °C; slicing; ultrathin sectioning; and staining. Finally, the sections were observed under a transmission electron microscope (TEM) (Philips, Amsterdam, Netherlands) at the Chongqing Medical University using standard techniques as described previously.

Golgi-Cox staining

Whole brains were harvested from female mice after ovariectomy. According to the manufacturer's instructions provided with the FD Rapid GolgiStain™ Kit (FD Neurotechnologies, Inc., USA), experimental animals were deeply anesthetized with 0.1% pentobarbital, and then brains were removed from the skull and rinsed in double distilled water to remove blood from the surface. Next, the brains were immersed in the impregnation solution, which was made by mixing equal volumes of solutions A and B, for 2 weeks at room temperature in the dark. Then, the brains were transferred into solution C and kept in the dark at room temperature for at least 72 h (up to 1 week). After that, brain sections were cut on a freezing microtome (CM1860; Leica, Wetzlar, Germany). Coronal sections (100 μm thick) were cut and transferred to gelatin-coated slides onto small drops of solution C. The staining procedure was closely followed: the sections were washed, dried, dehydrated with gradient ethanol, cleared with xylene, and permeabilized for coverslipping. Finally, the brain sections were imaged with a Leica DM 4000 microscope (Leica, Wetzlar, Germany).

Western blot

Brain tissue samples were lysed in RIPA lysis buffer (P0013B, Beyotime, Shanghai, China) and phenylmethanesulfonyl fluoride (PMSF, ST506, Beyotime) on ice. The lysates were separated by 8—12% Tris-glycine SDS-PAGE and electrotransferred to polyvinylidene difluoride (PVDF) membranes (0.45 μm pore size; IJ-58; Millipore, Darmstadt, Germany). Then, the membranes were blocked in 5% BSA for 2 h at 37 °C and incubated in primary antibodies at 4 °C overnight (Table 2). The next day, after washing in PBST three times, the membranes were incubated in secondary antibodies from the same species at 37 °C for 1 h. After three more washes with PBST, the immunoreactive bands were visualized by enhanced chemiluminescence (ECL, 4Awoll-100; 4A Biotech Co., Ltd., Beijing, China) and captured by the Molecular Imager ChemiDoc XRS System (731BR02996; Bio-Rad, Shanghai, China). Densitometry analysis was performed using Image Lab software (Bio-Rad, Hercules, USA).

Statistical analysis

All statistical analyses were performed with GraphPad Prism software (version 5.0). Data are expressed as the

Table 2 Information of primary antibodies in western blot.

Antibody Name	Antibody Source	Catalog number	Manufacturer	Dilutions
CYP19A1	Rabbit mAb	#DF6884	Affinity	1/100—1/10,000
ERp	Rabbit mAb	ab3577	Abeam	1/800
GLUT1	Rabbit mAb	ab115730	Abeam	1/1000
GLUT3	Rabbit mAb	ab191071	Abeam	1/1000
NeuN	Rabbit mAb	#24307	CST	1/1000
MAP2	Rabbit mAb	#4542	CST	1/1000
IGF1	Rabbit mAb	NBP2-16929	Novus	1/800
GSK3 beta	Mouse mAb	ab93926	Abeam	1/500—1/2000
GSK3 beta (phospho S9)	Rabbit mAb	ab75814	Abeam	1/10,000—1/20,000
IGF1R	Rabbit mAb	NBP1-77,680	Novus	1/800
PSD95	Mouse mAb	ab2723	Abeam	1/200—1/1000
GAP43	Rabbit mAb	ab75810	Abeam	1/100,000—1/200,000
beta actin	Mouse mAb	#A5441	Sigma Aldrich	1/5000—1/10,000
GAPDH	Rabbit pAb	AF7021	Affinity	1/3000—1/30,000

*Effective concentrations or concentration ranges were observed in their corresponding structions.

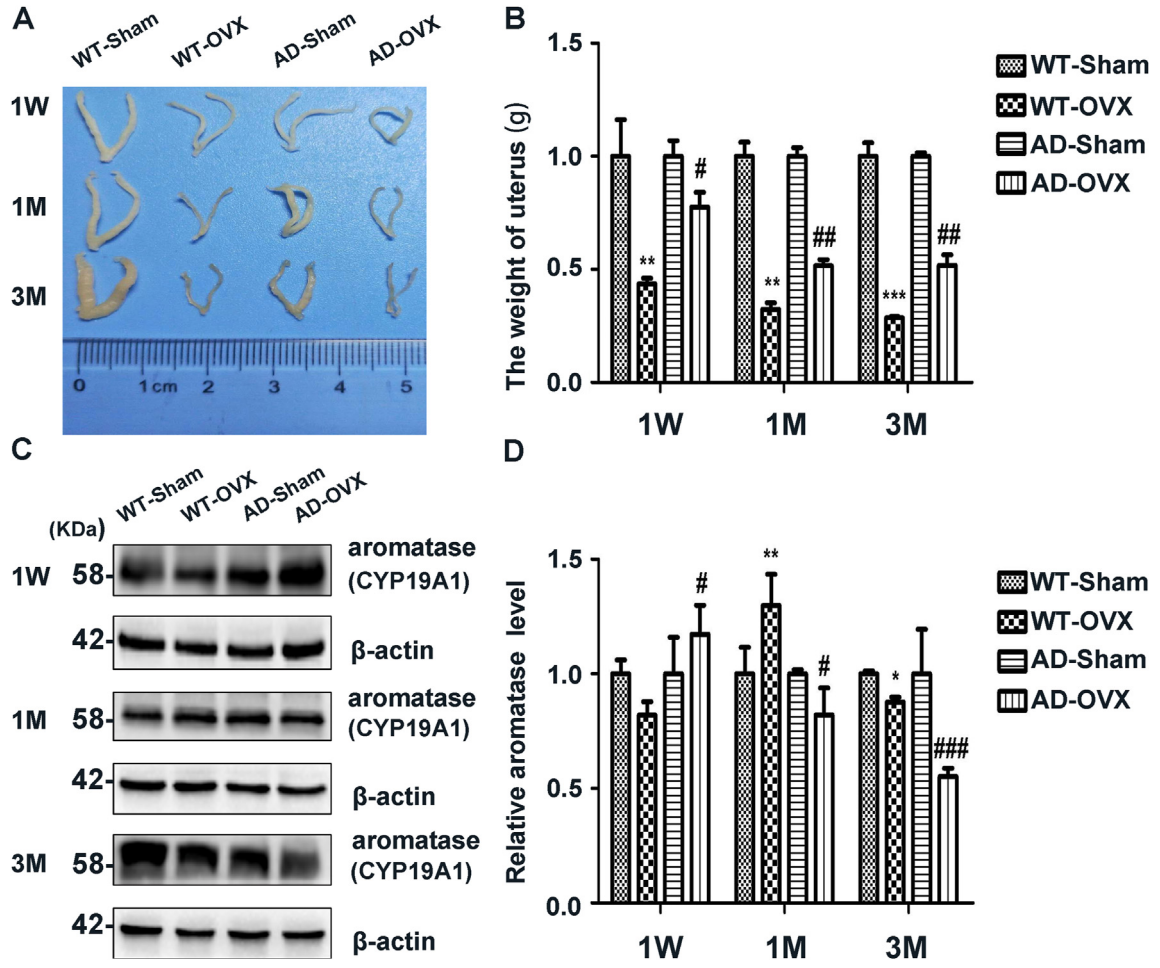

Figure 1 Estrogen levels in the circulation and brain of mice. **(A)** Image of uteri from all groups. **(B)** Quantification of uterus weight. **(C)** Western blot analysis of aromatase (CYP19A1) expression. β-actin was used as an internal control. **(D)** Densitometric analysis of CYP19A1 expression normalized to β-actin. Data are presented as the mean ± SEM. Compared with WT-Sham, $^{*}P < 0.05$, $^{**}P < 0.01$, $^{***}P < 0.001$; compared with AD-Sham, $\#P < 0.05$, $\#\#P < 0.1$, $\#\#\#P < 0.001$.

mean ± standard error of the mean (SEM). Statistically significant differences were determined by two-way analysis of variance (ANOVA) followed by the Bonferroni post hoc test or Student's *t*-test (for other comparisons between sham and OVX). $P < 0.05$ was considered statistically significant.

Results

Ovariectomy leads to estrogen deficiency in both the circulation and brain of mice

Three experimental models (1 week, 1 month, and 3 months) were designed to imitate human early postmenopause, middle postmenopause, and late postmenopause, respectively. Uterine weight was used as a bioassay to confirm depletion of ovarian hormones in mice. In both WT and AD mice, OVX induced a significant decrease in uterine weight compared with that in the sham groups (Fig. 1A, B). Next, the distribution of aromatase (CYP19A1), a key enzyme responsible for estrogen synthesis, in the mouse brain was studied. In this experiment, a compensatory increase in CYP19A1 protein expression was shown in the AD-OVX 1-week group, and significant decreases were found in the AD-OVX 1-month and 3-month groups (Fig. 1C, D). In WT mice, OVX induced a significant decrease in CYP19A1 expression only at 3 months (Fig. 1C, D). These results suggested that OVX can lead to a decrease in estrogen in both the circulation and the brain, and the change in brain estrogen in AD may be consistent with the level of circulating estrogen.

Estrogen deficiency causes cognitive impairments in mice

To examine the impact of OVX on spatial learning and memory, the Morris water maze test was performed. In hidden platform tests at 1 week after the OVX surgery, the escape latencies and path lengths were not significantly different between the OVX and sham groups (Fig. 2A, B). Mice in the OVX groups began to exhibit learning and memory impairment 1 month after the surgery, and AD-OVX mice showed longer escape latencies and path lengths to escape onto the hidden platform on the fourth and fifth

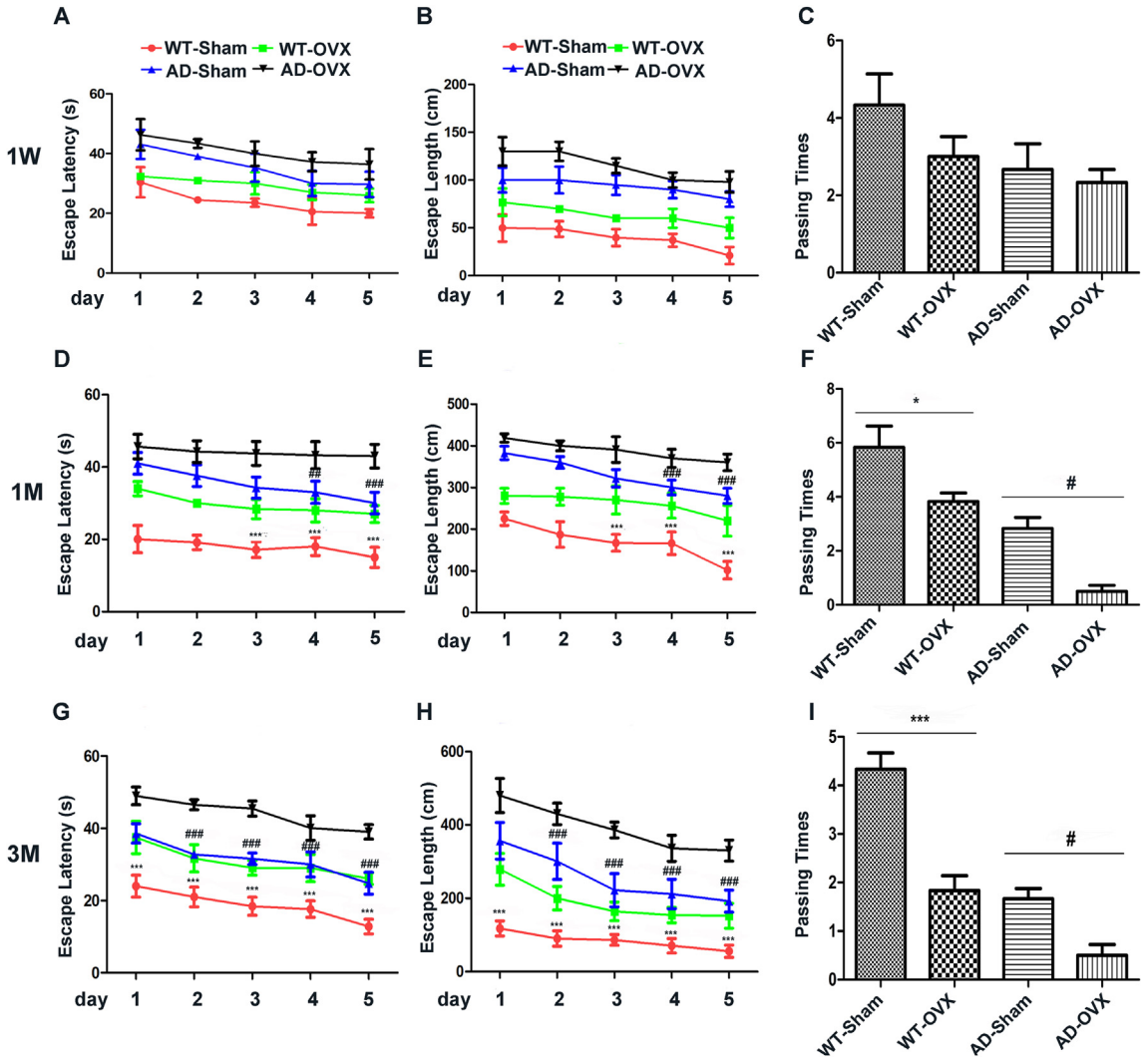

Figure 2 Estrogen deficiency causes learning and memory impairments in mice. **(A, B)** The escape latencies and path lengths of mice in hidden platform tests at 1 week after OVX. **(C)** In the probe trial, the OVX groups exhibited platform-passing times similar to those of the sham groups at 1 week after the surgery ($P > 0.05$). **(D, E)** The escape latencies and path lengths of mice in hidden platform tests at 1 month after OVX. **(F)** OVX mice at 1 month after surgery had fewer platform-passing times than sham-treated mice ($P < 0.05$). **(G, H)** The escape latencies and path lengths of mice in hidden platform tests at 3 months after OVX. **(I)** OVX mice at 3 months after surgery mice had significantly fewer platform-passing times than sham-treated mice ($P < 0.05$). Data are presented as the mean ± SEM. Compared with WT-Sham,*$P < 0.05$, **$P < 0.01$, ***$P < 0.001$; compared with AD-Sham, #$P < 0.05$, ##$P < 0.1$, ###$P < 0.001$ ($n = 6$).

days (Fig. 2D, E). The deficits were increased at 3 months after ovariectomy (Fig. 2G, H). In the spatial probe trial on the last day, the platform was removed. At 1 week after the surgery, AD-OVX mice exhibited platform-passing times similar to those of the sham group (Fig. 2C). In the 1-month and 3-month groups, AD-OVX mice had significantly fewer platform-passing times than sham-treated mice (Fig. 2F, I). In both the hidden platform tests and spatial probe trial, the WT-OVX group showed tendencies similar to those of the AD-OVX group (Fig. 2F, I). These data suggested that prolonged estrogen deficiency exacerbated cognitive deficits in female AD mice.

Estrogen deficiency increases neuritic plaques in the brain

To investigate whether OVX could exacerbate the pathology of AD, 4G8 immunochemical staining was used to detect Aβ-containing neuritic plaques in mouse brains and human AD brains. There were no Aβ plaques in the WT groups; furthermore, plaques were first observed in mice in the OVX 3-month groups (Fig. 3A). Additionally, there was a significant increase in plaque formation in AD mouse brains and human AD brains relative to that in the respective normal controls (Fig. 3B). Quantitative analysis showed that the Aβ

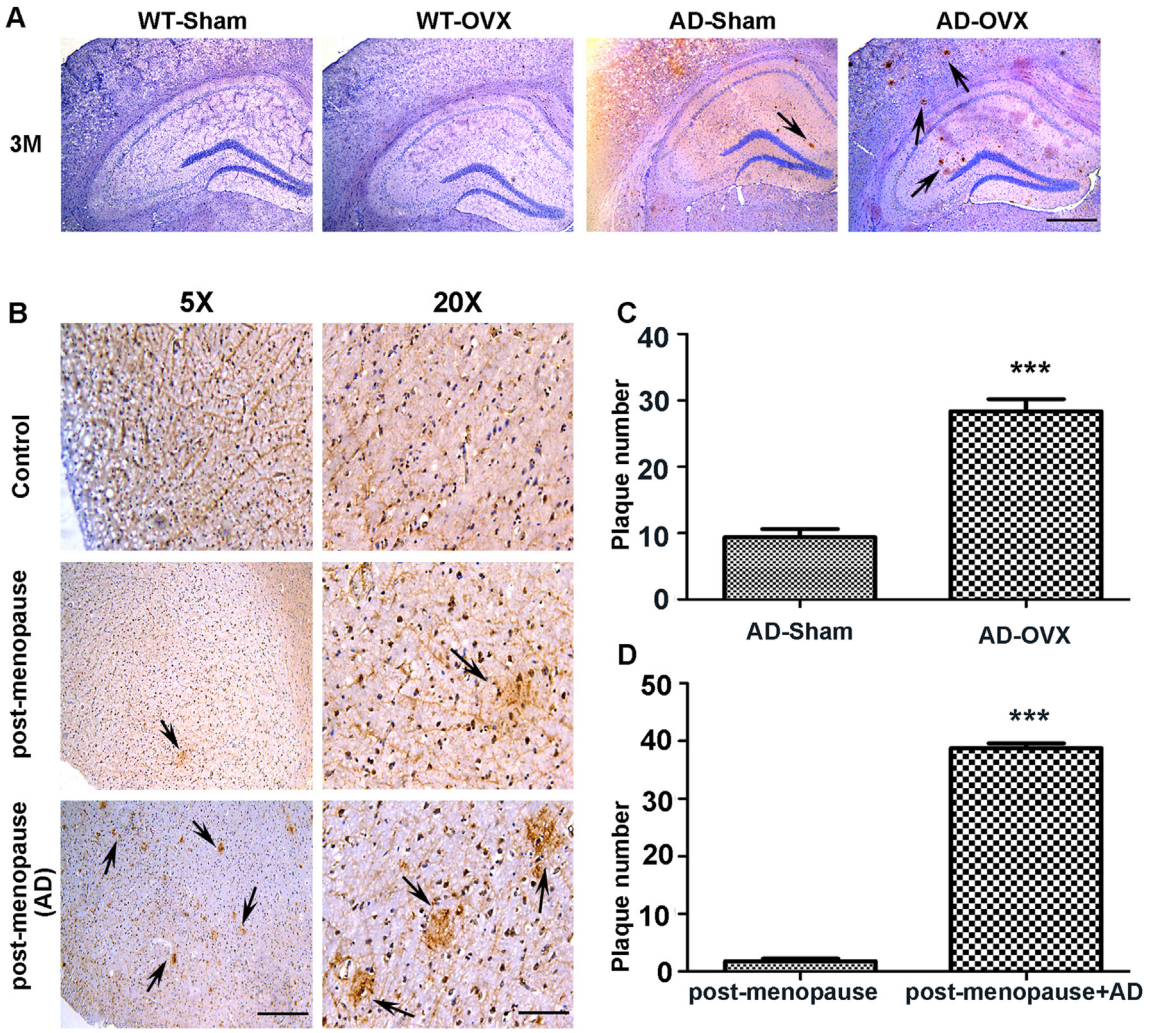

Figure 3 Estrogen deficiency increases neuritic plaques in the brain. Immunohistochemical staining of Aβ plaques (4G8) in mouse **(A)** and human **(B)** brain tissues. Quantification of the number of neuritic plaques in the mouse **(C)** and human **(D)** brains. Scale bar in A = 500 μm; Scale bars in B = 500 μm & 100 μm. The black arrows indicate plaques. Data are presented as the mean ± SEM. ***$P < 0.001$.

plaque number and burden were significantly increased in the cortex and hippocampus of the 3-month AD-OVX group compared with those of the AD-Sham group (Fig. 3C). The number of neuritic plaques in human menopausal AD female brains was obviously greater than that in the control brains (Fig. 3D). These results suggested that long-term ovarian hormone deprivation induced the deposition of neuritic plaques in the brains of AD patients.

Estrogen deficiency exacerbates hippocampal neuron loss in mice

To further examine the effects of the loss of ovarian hormones on neuronal morphology and protein levels, immunohistochemical staining and western blotting of the neuronal-associated markers MAP2 and NeuN were performed. The results revealed that the number of MAP2-positive cells in the hippocampus and the level of NeuN protein expression were increased in the OVX 1-week groups compared to the age-matched sham groups (Fig. 4A, a—d, B, C). In the OVX 1-month and 3-month groups, these changes occurred in both the hippocampus and cortex (Fig. 4A, e—l, B, C). These data indicated that long-term estrogen deficiency facilitated neuronal loss in the brains of AD mice.

Estrogen deficiency reduces the number of hippocampal dendritic spines in mice

Golgi-Cox staining was used to study neuron morphology in the dentate gyrus (DG) of the hippocampus, which is a part of the limbic system of the brain and is a key brain region related to learning and memory.[22] First, the number of dendrites per neuron was compared, and there was no difference between the OVX group and the sham group at 1 week after OVX (Fig. 5A, D). However, notably, dendrite number was decreased in the 1-month and 3-month OVX

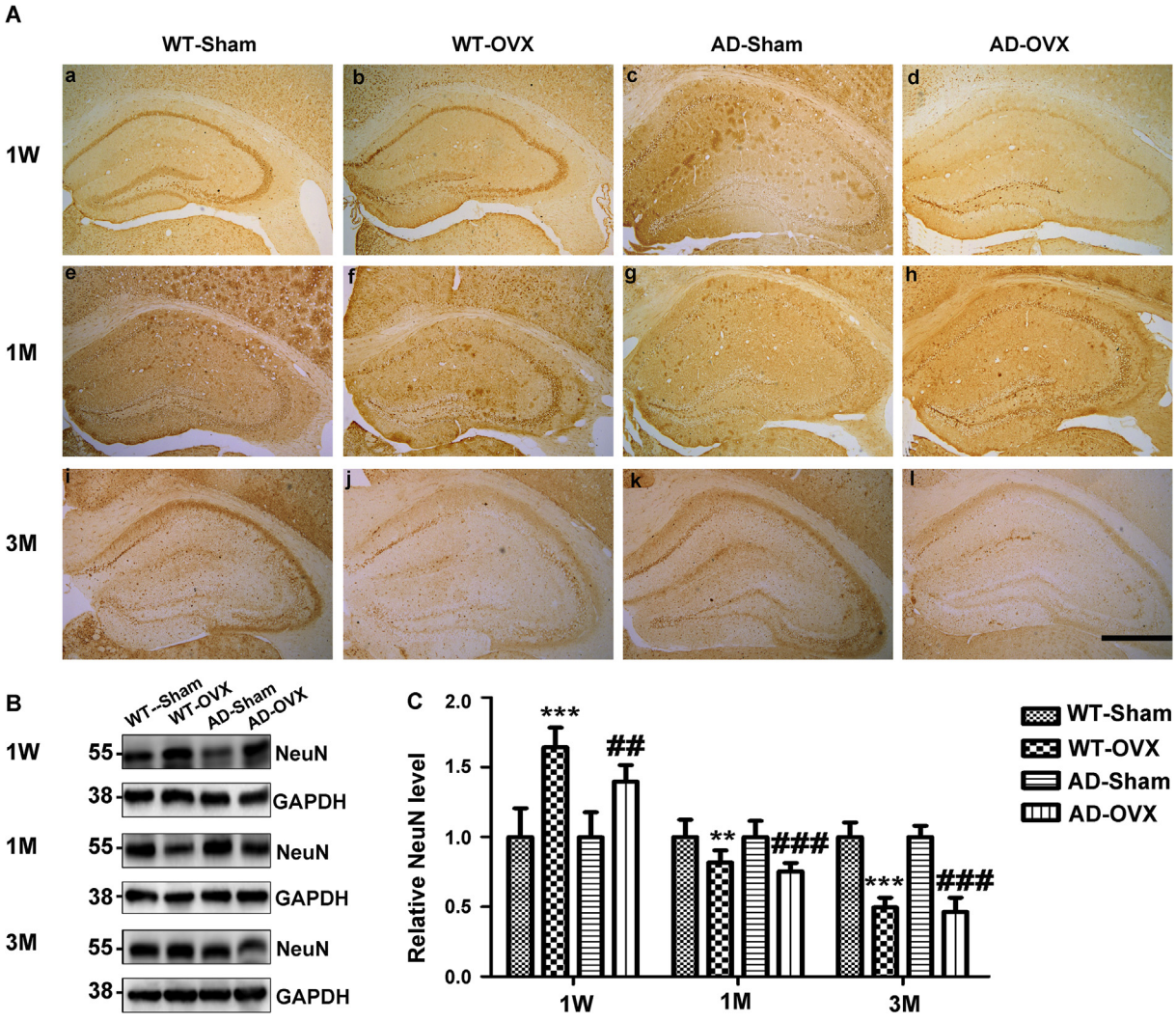

Figure 4 Estrogen deficiency exacerbates hippocampal neuron loss in mice. **(A)** Immunohistochemical staining of neuronal (MAP2) morphology in mouse brain. Scale bar = 500 μm. **(B)** Western blot analysis of NeuN expression. GAPDH was used as an internal control. **(C)** Densitometric analysis of NeuN expression normalized to GAPDH. Data are presented as the mean ± SEM. Compared with WT-Sham,*$P < 0.05$, **$P < 0.01$, ***$P < 0.001$; compared with AD-Sham, #$P < 0.05$, ##$P < 0.1$, ###$P < 0.001$.

groups (Fig. 5B—D). Next, the dendritic spine numbers were assessed, and no obvious morphological changes were observed between the OVX group and the sham group at 1 week after OVX (Fig. 5A, E). The statistical analysis showed that the numbers of dendritic spines in the 1-month OVX groups declined relative to those in the sham groups (Fig. 5A, E), and more pronounced declines in dendritic spine number were shown in the 3-month OVX groups (Fig. 5C, E). These results suggested that long-term estrogen deficiency reduced the number of dendritic spines in the hippocampus of AD mice.

Estrogen deficiency damages the hippocampal synaptic structure of mice

Learning and memory are associated with biochemical and morphological changes at the synaptic level. OVX leads to spatial learning and memory deficits in mice. Therefore, transmission electron microscopy (TEM) was used to observe the synaptic structure in the hippocampus (Fig. 6.1A). The results revealed that the number of synapses in the hippocampus was not significantly different between the AD-OVX group and the respective sham group at 1 week after OVX (Fig. 6.1B). However, the number of synapses in the hippocampus was significantly increased in the WT-OVX group compared to the WT-Sham group (Fig. 6.1B). At 1 and 3 months after OVX surgery, the synapse numbers in the hippocampus were significantly decreased in both AD and WT mice compared with the respective sham-treated mice (Fig. 6.1B). The number of presynaptic vesicles was markedly decreased only in the 3-month AD-OVX female mice (Fig. 6.1C). This change occurred earlier in the WT-OVX group at 1 month (Fig. 6.1C). TEM analysis showed that the length of the synaptic active zone was increased in the 1-week OVX group (Fig. 6.1D). However, a significant decrease was found in the 1- and 3-month OVX female mouse groups (Fig. 6.1D). The levels of the synapse-related proteins GAP43 and PSD-95 were further analyzed by western

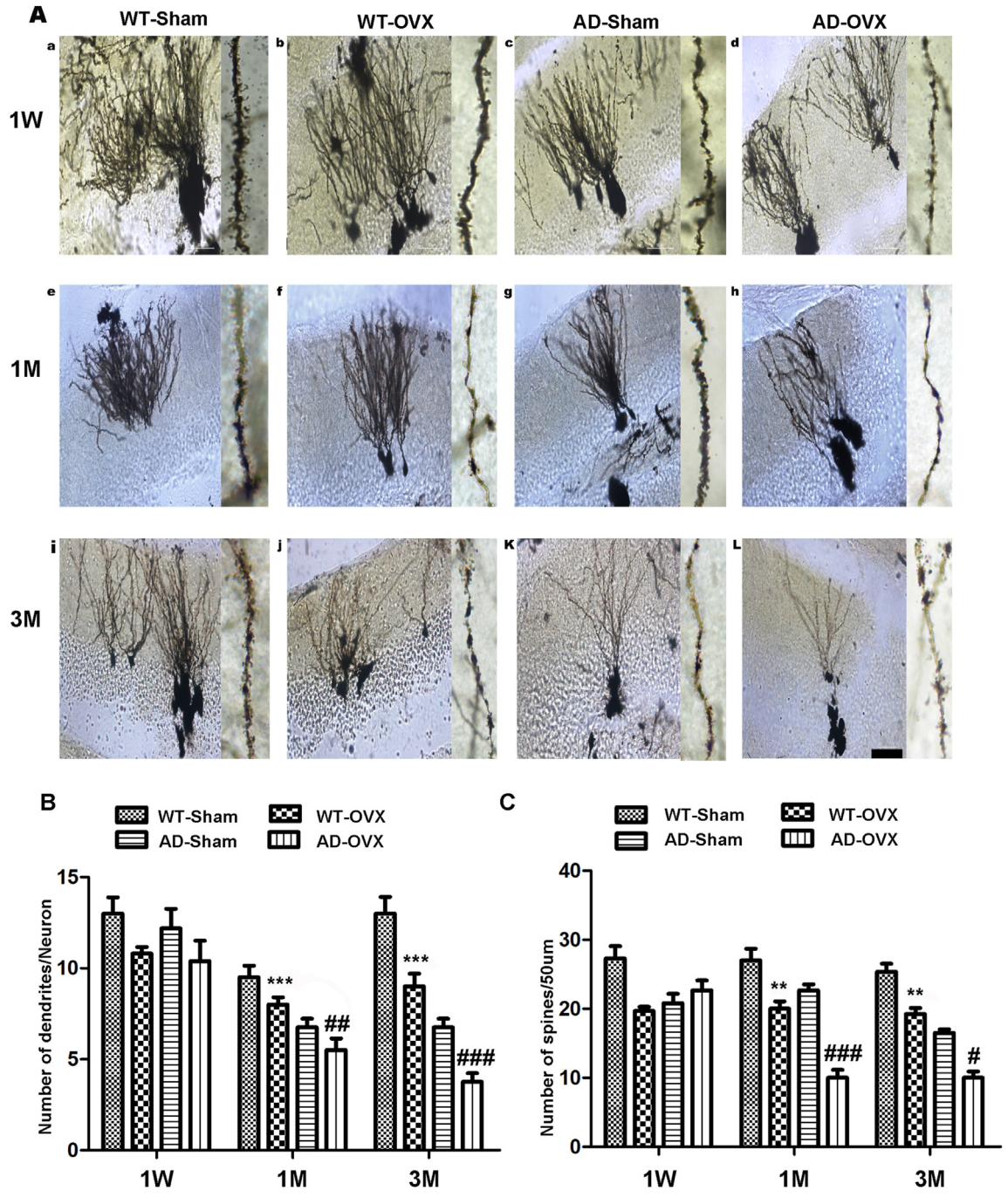

Figure 5 Estrogen deficiency reduces the number of hippocampal dendritic spines in mice. **(A)** Dendrites (Scale bar = 200 μm) and dendritic spines were observed by Golgi staining. **(B, C)** Quantitative analysis of the numbers of dendrites and dendritic spines. Data are presented as the mean ± SEM. Compared with WT-Sham,*$P < 0.05$, **$P < 0.01$, ***$P < 0.001$; compared with AD-Sham, #$P < 0.05$, ##$P < 0.1$, ###$P < 0.001$.

blotting. GAP43 and PSD95 protein expression levels in 1-week OVX 2xTgAD female mouse brains were not significantly different from those in sham mouse brains (Fig. 6.2A). However, there was an upward trend in GAP43 and PSD95 protein expression in the WT-OVX groups, and the difference was statistically significant (Fig. 6.2B, C). The expression levels of GAP43 and PSD95 in the 1- and 3-month OVX groups significantly decreased compared with those in the sham groups (Fig. 6.2B, C). These results suggested that long-term estrogen deficiency can cause the destruction of hippocampal synapses.

Estrogen deficiency downregulated glucose transport proteins in the brains of mice

The earliest defect in the pathological progression of AD is associated with impaired energy metabolism.[23,24] The

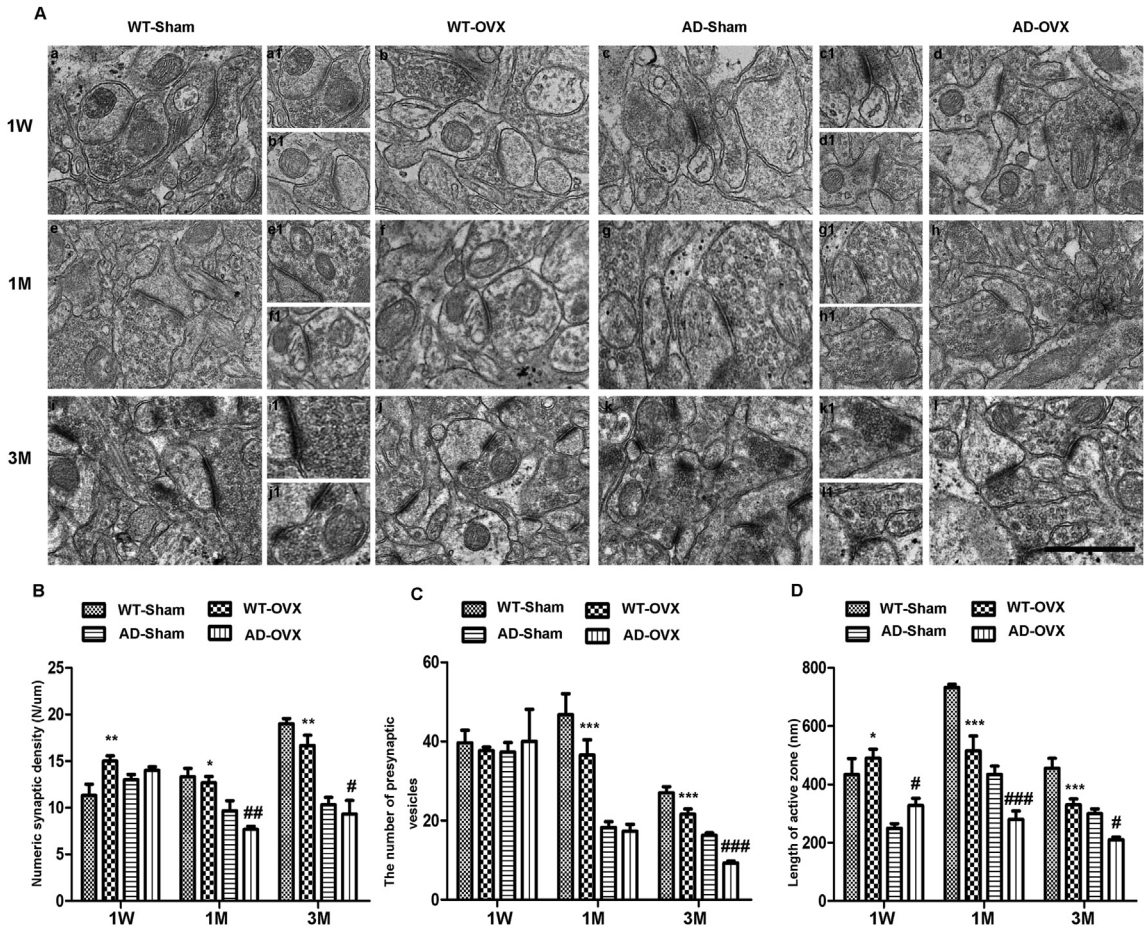

Figure 6.1 Estrogen deficiency damages hippocampal synaptic structure in mice. **(A)** Observation of synaptic changes in the mouse hippocampus by TEM. Scale bar = 1 μm. **(B—D)** The numbers of synapses and presynaptic vesicles and the lengths of synaptic active zones in the hippocampal region of mice were quantitatively analyzed. Data are presented as the mean ± SEM. Compared with WT-Sham,*$P < 0.05$, **$P < 0.01$, ***$P < 0.001$; compared with AD-Sham, #$P < 0.05$, ##$P < 0.1$, ###$P < 0.001$.

cellular energy of brain metabolism comes from glucose metabolism, and impaired cerebral glucose metabolism is one of the most important clinical and biochemical characteristics leading to AD. Thus, the levels of glucose transporters in the brain were measured by western blotting. The results showed that the protein levels of the glucose transporters GLUT-1 and GLUT-3 in the AD-OVX group were significantly higher than those in the AD-Sham group 1 week after OVX, while 1 month and 3 months after OVX, the protein levels of the glucose transporters were significantly lower in the AD-OVX groups than in the AD-Sham groups; additionally, the same trend was observed in the WT groups (Fig. 7). These results suggested that long-term estrogen deficiency can down-regulate the protein expression of glucose transporters in the mouse brain.

Estrogen deficiency damages the mitochondrial ultrastructure of mice

Mitochondria are the key organelles of cellular energy metabolism. To investigate the impact of OVX on mitochondrial ultrastructure and function, TEM was used to observe their structure. The TEM images showed that there were no obvious abnormalities in mitochondrial structure in the early stage at 1 week after OVX (Fig. 8a—d). As the time after OVX was increased to 1 month, mitochondrial abnormalities began to appear (Fig. 8e—h). Notably, severe swelling occurred inside the mitochondria in the 3-month OVX group (Fig. 8i—l). Mitochondria were isolated from mouse brains. These results suggested that prolonged estrogen deficiency can damage the structure of mitochondria.

Estrogen deficiency induces abnormal upregulation of mitochondrial ERβ in mice

Estrogen functions by binding to estrogen receptors (ERs). ERβ is strongly expressed in the hippocampus and other cognition-related brain regions.[9,10] To investigate the impact of OVX on ERβ, we first assessed the level of ERβ in the whole brain. The statistical analysis showed that at 1 week after OVX, there were no significant differences between the OVX and sham groups in either WT or AD mice (Fig. 9A, E). At 1 month after OVX, loss of ovarian hormones induced a significant decrease in ERβ expression in both WT

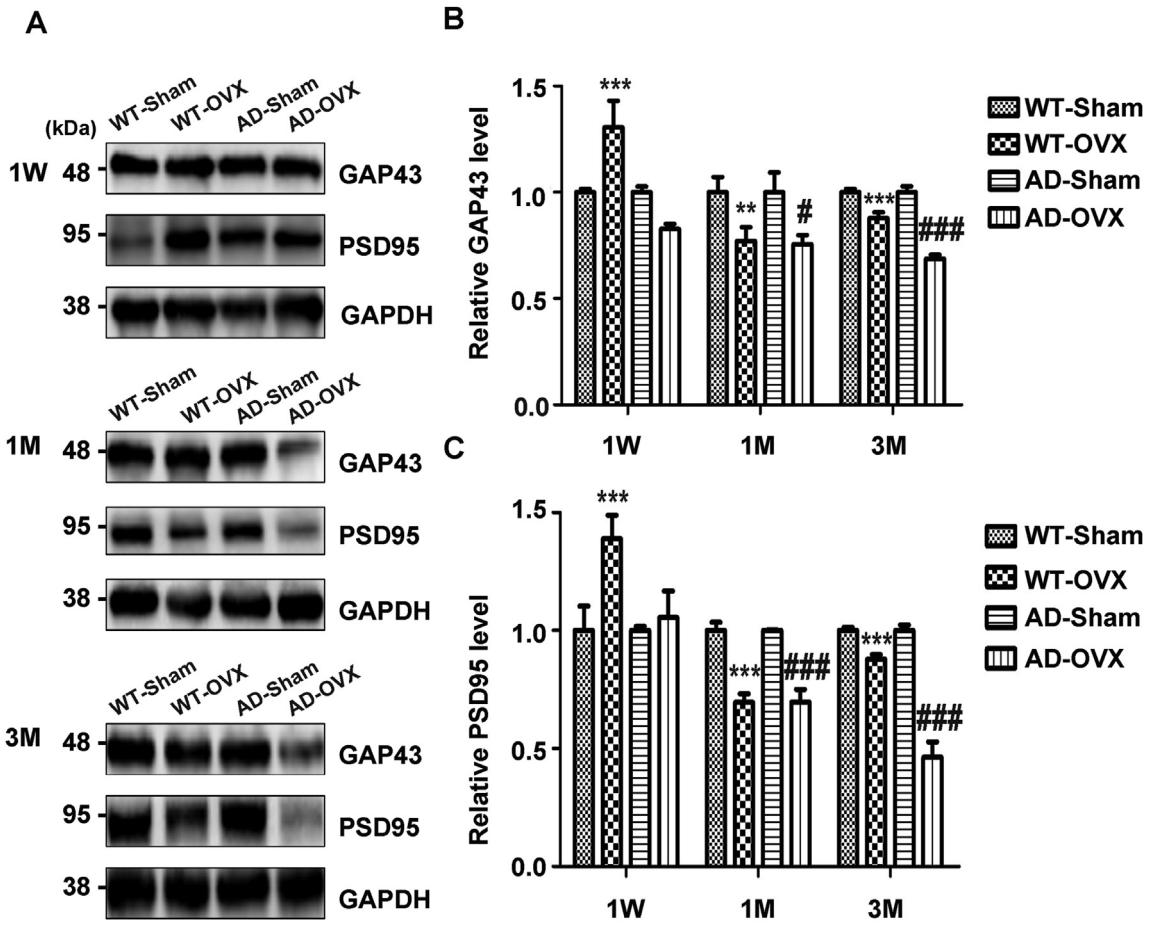

Figure 6.2 Estrogen deficiency downregulated synapse-related proteins in the mouse brain. **(A)** Western blot analysis of GAP43 and PSD95 expression. GAPDH was used as an internal control. **(B, C)** Densitometric analysis of GAP43 and PSD95 expression normalized to GAPDH. The expression levels of GAP43 and PSD95 in the 1- and 3-month OVX groups were significantly lower than those in the AD-Sham group. Data are presented as the mean ± SEM. Compared with WT-Sham,*$P < 0.05$, **$P < 0.01$, ***$P < 0.001$; compared with AD-Sham, #$P < 0.05$, ##$P < 0.1$, ###$P < 0.001$.

and AD female mice (Fig. 9A, B). At 3 months after OVX, there was a difference in the expression of ERβ between WT and AD mice. In WT mice, OVX induced a significant decrease in the level of ERβ. However, in AD mice, the difference in the level of ERβ in the OVX group and the sham group was not statistically significant (Fig. 9A, B). Next, mitochondria were isolated from mouse brain tissues, and the level of ERβ was assessed by Western blot. The statistical analysis showed that 1 week after OVX, there was a significant increase in mitochondrial ERβ (mt-ERβ) levels in the WT-OVX group compared to the WT-Sham group, but no significant difference was shown between the AD-OVX group and the AD-Sham group (Fig. 9C, D). One month after the surgical operation, significant decreases in mtERβ were observed in both WT-OVX and AD-OVX mice compared to the respective sham-treated mice (Fig. 9C, D). However, at three months after the surgery, long-term ovariectomy induced a significant increase in the mtERβ expression level in the OVX groups compared with the corresponding sham groups (Fig. 9C, D). These results suggested that long-term estrogen deficiency can induce abnormal upregulation of mt-ERβ expression in the brain tissue of AD mice.

Estrogen deficiency might regulate energy metabolism through the IGF-1/IGF-1R/GSK-3β signaling pathway

To understand the molecular basis of the effect of estrogen deficiency on brain energy metabolism, some molecules associated with energy metabolism signaling pathways were evaluated. The results showed that OVX induced significant increases in IGF-1, IGF-1R and the ratio of p-GSK3β to t-GSK-3β at 1 week after OVX. At 1 and 3 months after OVX, significant decreases in the levels of IGF-1 and IGF-1R and the ratio of p-GSK3β to t-GSK-3β were observed in the OVX groups compared to the corresponding sham groups (Fig. 10A–D). These results suggested that estrogen

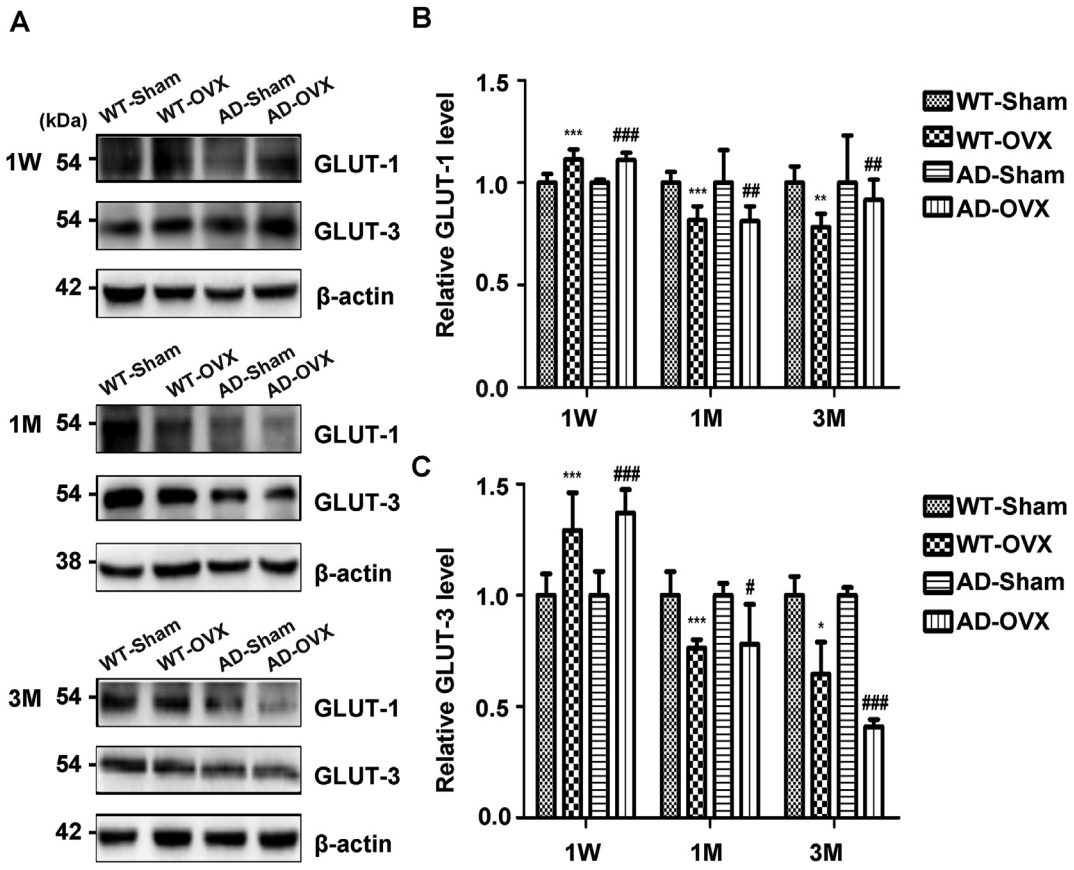

Figure 7 Estrogen deficiency downregulated glucose transport proteins in the mouse brain. **(A)** Western blot analysis of GLUT-1 and GLUT-3 expression. β-actin was used as an internal control. **(B, C)** Densitometric analysis of GLUT-1 and GLUT-3 expression normalized to β-actin. The brain expression levels of GLUT-1 and GLUT-3 in the 1- and 3-month OVX groups were significantly lower than those in the sham groups. Data are presented as the mean ± SEM. Compared with WT-Sham, $^{*}P < 0.05$, $^{**}P < 0.01$, $^{***}P < 0.001$; compared with AD-Sham, $\#P < 0.05$, $\#\#P < 0.1$, $\#\#\#P < 0.001$.

deficiency might regulate energy metabolism through the IGF-1/IGF-1R/GSK-3β signaling pathway.

Discussion

AD is a progressive age-related neurodegenerative disorder characterized by cognitive impairment.[25] The incidence of AD in women is 3 times higher than that in men of a comparable age.[26] Menopausal status increases the risk of dementia in women.[27] In addition, compared with men at the same stage of AD, postmenopausal women with AD have more severe cognitive impairments.[28] Previous studies have shown that estrogen can promote the growth and survival of memory-associated cholinergic neurons, inhibit the production and toxicity of Aβ, strengthen neuronutrition and reduce the hyperphosphorylation of tau.[29] Clinical studies have shown that estrogen replacement therapy can improve AD-related cognitive impairments and reduce the risk of AD in early menopausal women.[30,31] These findings indicate that estrogen plays an important role in AD. However, there is still a lack of systematic research on this issue, and the underlying mechanism is unclear. This study aimed to explore the effect of estrogen deficiency on the development and progression of AD to clarify the potential molecular mechanism. We hope to provide a new conceptual basis for investigating the pathogenesis of AD.

The APP/PS1 double transgenic mouse is a well-characterized AD mouse model. In OVX mice, the time points of six days and three months after OVX correspond to early and late postmenopause in women, respectively.[32,33] Therefore, mice at one week after OVX (simulating early postmenopause) and at one and three months after OVX (simulating middle and late postmenopause, respectively) were used in this study. Uterine weight is widely used as a bioassay to determine the levels of hormones produced by the ovaries.[34] The results in this study showed that the uterine weight of AD mice began to decrease one week after OVX. At one month and three months after OVX, the uterine weight was decreased significantly, indicating that OVX simulates decreased circulating estrogen levels. The change in estrogen in the brain was evaluated by detecting the expression of aromatase (CYP19A1), which is an enzyme that converts testosterone into estrogen.[35] The results showed that the expression of aromatase (CYP19A1) in the brain was increased one week after OVX but decreased one month and three months after surgery. These results suggest that compensatory regulation may occur,[36] and changes in brain estrogen levels may be consistent with changes in peripheral estrogen levels.

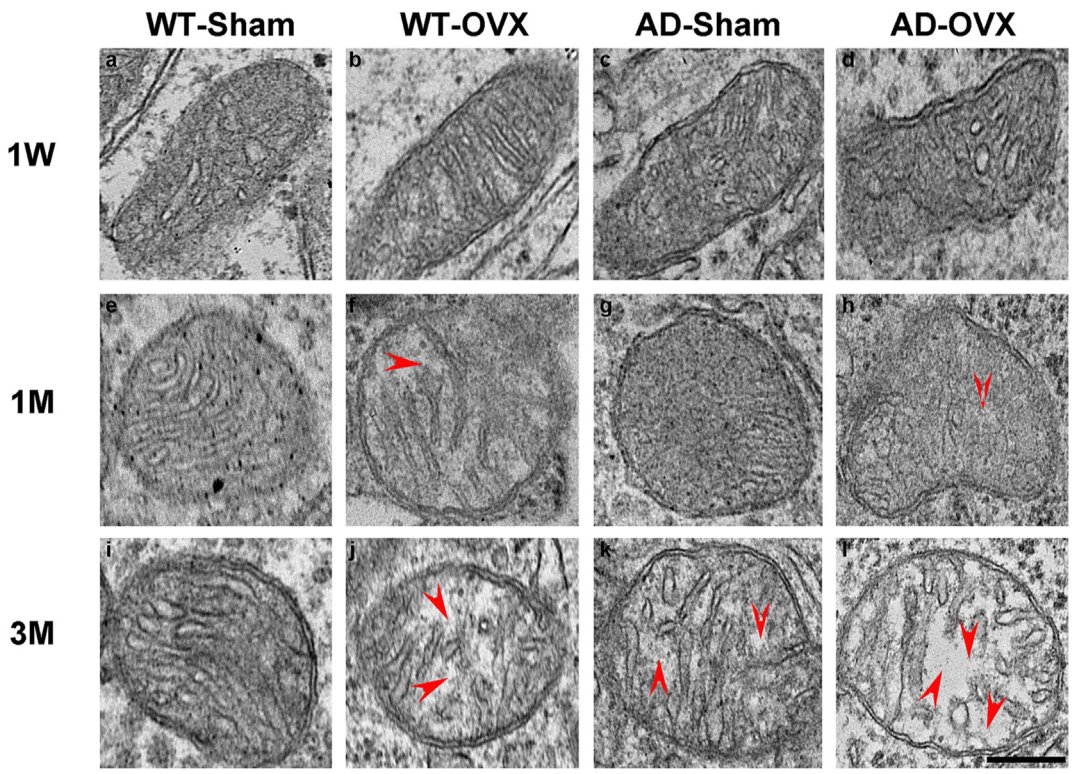

Figure 8 Estrogen deficiency damages mitochondrial ultrastructure in mice. Observation of mitochondrial ultrastructure by TEM. The results showed that there were no obvious mitochondrial abnormalities in the brain of OVX mice 1 week after surgery. Severe mitochondrial swelling occurred in the 1- and 3-month OVX groups. Scale bar = 500 nm; red arrows indicate swelling.

According to recent research, estrogen in the brain is a new type of neuroregulator that may play a role in synaptic plasticity and learning and memory formation. Studies have shown that mice with decreased brain estrogen levels had deficits in spatial memory and cognitive and situational fear memory, and memory impairments improved when estrogen levels were restored.[37] This study observed changes in the learning and memory of mice induced by estrogen deficiency for different time periods. The results showed that long-term estrogen deficiency promoted the impairment of learning and memory in mice, which is consistent with previous reports. However, it remains unknown why estrogen deficiency causes cognitive impairment.

The classical pathological features of AD include senile plaques formed by extracellular Aβ deposition, neurofibrillary tangles (NFTs) formed by intracellular tau hyperphosphorylation, and the synaptic reduction, degeneration and loss of memory-related neurons.[37] Clinical studies have confirmed that the accumulation of Aβ can cause NFTs, synaptic damage and neuronal apoptosis in the brains of AD mice.[38,39] The results of our study showed that there were no SPs in the brains of AD mice at one week or at one month after OVX, but obvious SPs appeared at three months after OVX. The reason for these results may be related to the characteristics of this animal model and age-related factors. Furthermore, we detected SPs in the brains of postmenopausal women with AD, which was consistent with an earlier report.[40] As described in the results section, we confirmed that long-term estrogen deficiency can cause neuron loss, and further experiments also confirmed structural changes in the brain. These results verified that estrogen deficiency caused pathological changes in the AD mouse brain.

Synapses and dendritic spines are dynamic structures, and their plasticity is considered to be the basis of learning and memory.[41] It has been reported that synaptic density and dendritic spines were decreased significantly in AD patient brains, especially in the cortex and hippocampus, and the loss of dendritic spines was correlated with a low emotional state.[42,43] However, there is still a lack of research on the structural basis of learning and memory impairment caused by estrogen deficiency. In this study, the dynamic changes in synapses and dendritic spines in mice after OVX were observed in detail. The results showed that long-term estrogen deficiency caused the loss of synapses and dendritic spines in AD and WT mice. To some extent, these results enrich the evidence of structural changes in learning and memory after OVX. Thus, it has been shown that long-term estrogen deficiency causes cognitive impairments by altering the structure of the brain.

Studies have shown that the earliest defect in the pathological progression of AD is the impairment of energy metabolism.[44–47] Glucose metabolism provides the main energy source for biological activities. Many studies have proven that impaired brain glucose metabolism is one of the most important biochemical characteristics of AD.[48,49] Estrogen is beneficial to the biological energy system of the brain,[50] and estrogen depletion affects glucose

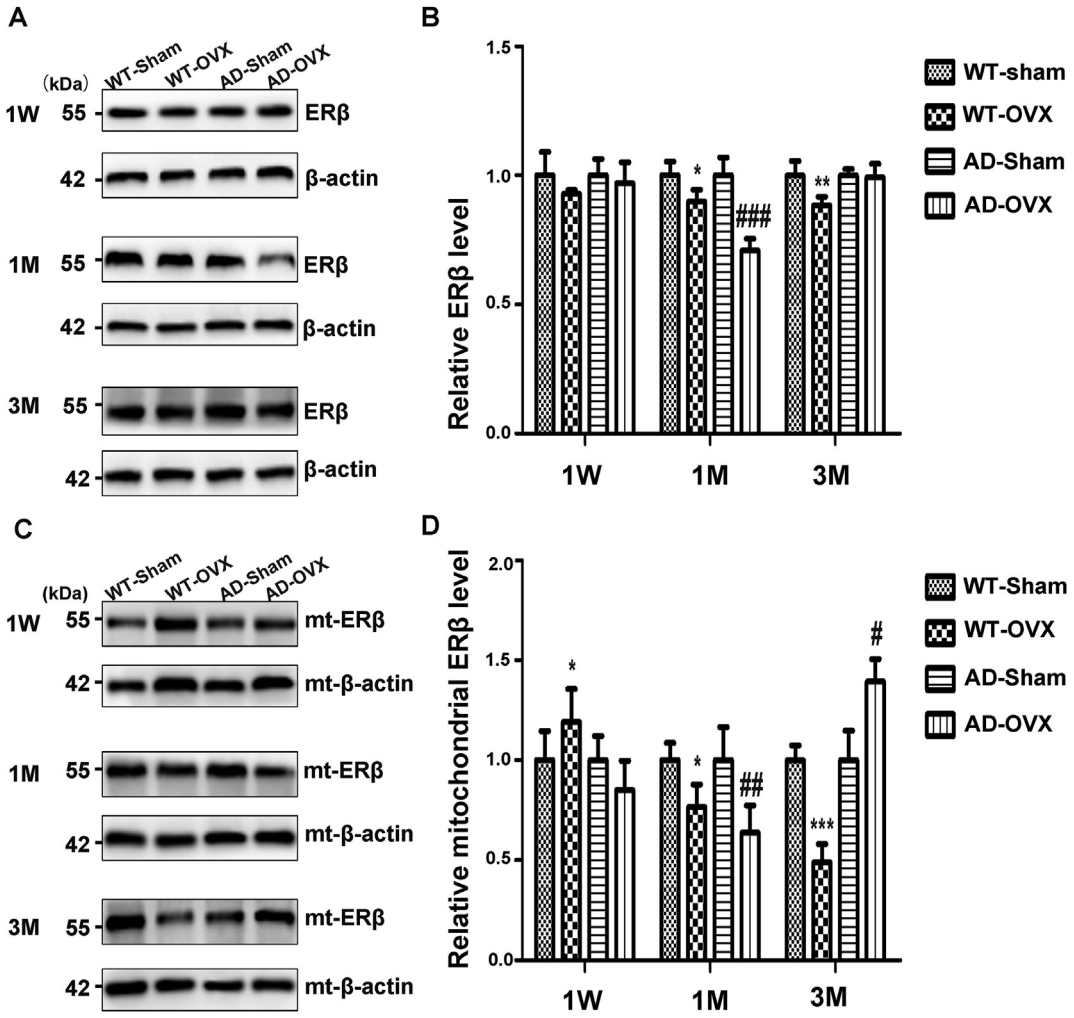

Figure 9 Estrogen deficiency induces abnormal upregulation of mitochondrial ERβ in mice. **(A)** Western blot analysis of total ERβ expression in the brain. β-actin was used as an internal control. **(B)** Densitometric analysis of ERβ expression normalized to β-actin. **(C)** Western blot analysis of ERβ expression in mitochondria. β-actin was used as an internal control. **(D)** Densitometric analysis of ERβ and mt-ERβ expression normalized to β-actin. Data are presented as the mean ± SEM. Compared with WT-Sham, $^{*}P < 0.05$, $^{**}P < 0.01$, $^{***}P < 0.001$; compared with AD-Sham, $\#P < 0.05$, $\#\#P < 0.1$, $\#\#\#P < 0.001$.

metabolism.[51] Glucose uptake by cells to provide energy for the brain is mediated by glucose transporters. Two types of glucose transporters (GLUT-1 and GLUT-3) are present in the membranes of brain endothelial cells, astrocytes, and neurons.[52] GLUT-1 is a low-affinity transporter, but it is highly sensitive to changes in glucose levels. GLUT-3 is a high-affinity transporter expressed on the neuronal membrane that facilitates glucose transport into neurons. Our results showed that in the brain, GLUT-1 and GLUT-3 were increased in the early stage of OVX but decreased in the middle and late menopausal stages. This trend was consistent with previous reports.[53,54] Glucose metabolism depends on glucose uptake by the cells. Therefore, a decrease in glucose transporters reflects a decrease in glucose metabolism.

Mitochondria are the main sites of energy metabolism. There is growing evidence that mitochondrial dysfunction is closely related to age-related neurodegenerative diseases, including AD.[48,49,51] It was reported that mitochondrial energy metabolism disorder predated the appearance of pathological features in AD female mice. In the present study, we observed the mitochondrial ultrastructure by transmission electron microscopy, and the results showed that the structure of brain mitochondria was disordered after bilateral ovariectomy in mice. The structural abnormalities became increasingly obvious with time. Thus, it can be speculated that mitochondrial structural abnormalities led to impaired energy metabolism, and estrogen deficiency was one of the causes of abnormal mitochondrial structure. Thus, we hypothesized that the mitochondrion could be a target organelle of estrogen.

Estrogen binds to its receptor and then exerts its biological effects. The classic estrogen receptors (ERs) include two subtypes: ERα and ERβ. In the brain, ERα is highly expressed in regions related to reproductive regulation, such as the hypothalamus and the bed nucleus of the stria terminalis, while ERβ is strongly

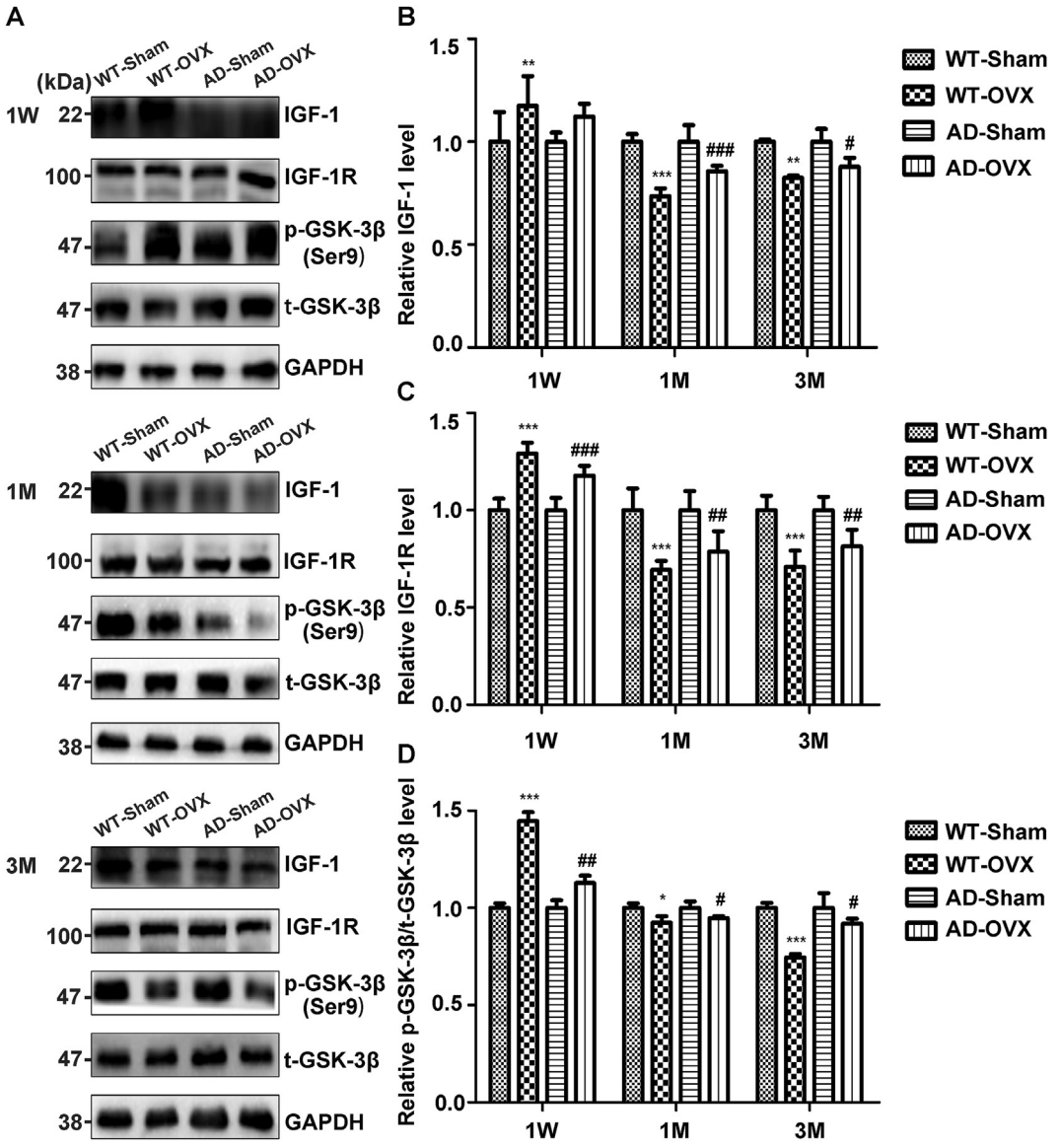

Figure 10 Estrogen deficiency inhibits IGF-1 activity and stimulates the GSK-3β signaling pathway. **(A)** Western blot analysis of IGF-1, IGF-1R, GSK-3β and p-GSK-3β(Ser9) expression. GAPDH was used as an internal control. **(B, C)** Densitometric analysis of IGF-1 and IGF-1R expression normalized to GAPDH. **(D)** Quantitative analysis of relative GSK-3β and p-GSK-3β (Ser9) levels. Data are presented as the mean ± SEM. Compared with WT-Sham, $^{*}P < 0.05$, $^{**}P < 0.01$, $^{***}P < 0.001$; compared with AD-Sham, $\#P < 0.05$, $\#\#P < 0.1$, $\#\#\#P < 0.001$.

expressed in the olfactory bulb, basal forebrain, cerebral cortex, hippocampus and other brain areas closely related to learning and memory.[9,10] Many studies have confirmed the existence of mitochondrial ER, and in the brain, ERβ is mainly located in mitochondria.[11,12] It seems that estrogen works by binding to mitochondrial ERβ (mt-ERβ). We detected the expression levels of brain ERβ and mitochondrial ERβ. Our data suggested that abnormal upregulation of ERβ occurred with prolonged estrogen deficiency. Moreover, a lack of estrogen causes low levels of hormone-receptor complex formation, leading to a low biological effect of estrogen. In the end, the low rate of hormone-receptor complex formation may cause aberrant accumulation of ERβ, which may impair the function of mitochondria.

It has been reported that mt-ERβ in neurons regulates energy metabolism, and mt-ERβ deficiency in AD is related to mitochondrial dysfunction.[55] ERβ is not only distributed in neurons but also expressed in glial cells.[56] Based on the distribution of ERβ and considering our results and those of other studies, we speculate that the increased protein level of mt-ERβ after OVX may be due to mt-ERβ production by glial cells and that the mt-ERβ in glial cells may perform different functions than those of mt-ERβ in neurons and may even perform the opposite function, which may exacerbate energy metabolism dysfunction and pathological changes in AD.

Further bioinformatics analysis of the gene network showed that insulin-like growth factor-1 (IGF-1) was the core promoter in early hippocampal energy metabolism. Its

receptor, IGF-1R, was strongly expressed in the dentate gyrus and CA2~CA3 regions of the hippocampus. Studies have shown that IGF-1 plays an important role in regulating the energy metabolism of nerve cells.[57] Likewise, in this study, we found that as the duration of estrogen deficiency increased, the expression levels of IGF-1 and IGF-1R in the OVX groups decreased significantly compared to those in the sham groups. This finding suggests that energy metabolism disorders caused by estrogen deficiency may be related to the IGF-1 signaling pathway. Moreover, it has been reported that IGF-1 signal transduction defects involve the phosphatidylinositol 3-kinase (PI3K)/Akt pathway and produce harmful cascade reactions in glucose metabolism, and the downstream target protein glycogen synthase kinase-3β (GSK-3β) is closely related to the characteristic pathological changes of AD.[21] GSK-3β is one of the two isoforms of GSK-3, which have similar functions; the other isoform is GSK-3α. A large proportion of GSK-3β is located in the cytoplasm, and a small proportion of cytoplasmic GSK-3β is located in mitochondria and the nucleus, while GSK-3α is not detected in mitochondria.[58] However, experiments with SH-SY5Y cells have shown that the activity of GSK-3β in mitochondria and the nucleus is 5—8 times higher than that in the cytoplasm.[59] GSK-3β is a substrate of various signaling pathways. GSK-3β also plays an important role in the regulation of mitochondrial bioenergetic metabolism.[60] Inhibitory phosphorylation at the Ser9 site inactivates GSK-3β.[61] In our research, the proportion of pSer9-GSK-3β and GSK-3β decreased significantly in the middle and late stages of estrogen deficiency. These results suggest that abnormal activity of GSK-3β is involved in the occurrence of AD and causes mitochondrial energy disorders.

In summary, it can be inferred from our findings that long-term estrogen deficiency causes aberrant accumulation or upregulation of mitochondrial ERβ, which mediates energy metabolism disorders. This causes pathological changes in the AD brain that in turn lead to learning and memory impairment. These changes may occur through a mechanism in which mt-ERβ mediates an IGF-1 energy metabolism signaling pathway, namely, the IGF-1/IGF-1R/GSK-3β signaling pathway. The results of this study might provide innovative ideas for the effective prevention and treatment of AD.

Author contributions

Guiqiong He: concept and design, supervision; **Min Luo:** literature search, experimental studies, writing original draft preparation; **Qinghua Zeng:** experimental studies, manuscript editing and reviewing; **Kai Jiang** and **Yueyang Zhao:** software; **Zhimin Long:** data analysis; **Yexiang Du:** data acquisition; **Kejian Wang:** concept and resources support.

Conflict of interests

The authors declare that they have no known competing financial interests or personal relationships that could have appeared to influence the work reported in this paper.

Funding

This study was supported by the National Natural Science Foundation of China (No. 81671257, 81371221, and 31600825) and the Innovation Research Group at Institutions of Higher Education in Chongqing (No. CXQTP19019019034).

References

1. Grøntvedt GR, Schröder TN, Sando SB, White L, Bråthen G, Doeller CF. Alzheimer's disease. *Curr Biol*. 2018;28(11):R645—R649.
2. Carrillo MC, Dean RA, Nicolas F, et al. Revisiting the framework of the national Institute on aging-Alzheimer's association diagnostic criteria. *Alzheimers Dement*. 2013;9(5):594—601.
3. Ameen-Ali KE, Wharton SB, Simpson JE, Heath PR, Sharp P, Berwick J. Review: neuropathology and behavioural features of transgenic murine models of Alzheimer's disease. *Neuropathol Appl Neurobiol*. 2017;43(7):553—570.
4. Schroeder JP, Packard MG. Systemic or intra-amygdala injections of glucose facilitate memory consolidation for extinction of drug-induced conditioned reward. *Eur J Neurosci*. 2003;17(7):1482—1488.
5. Foster KA, Margraf RR, Turner DA. NADH hyperoxidation correlates with enhanced susceptibility of aged rats to hypoxia. *Neurobiol Aging*. 2008;29(4):598—613.
6. Yun J, Yeo IJ, Hwang CJ, et al. Estrogen deficiency exacerbates Aβ-induced memory impairment through enhancement of neuroinflammation, amyloidogenesis and NF-κB activation in ovariectomized mice. *Brain Behav Immun*. 2018;73:282—293.
7. Simpkins JW, Yang SH, Wen Y, Singh M. Estrogens, progestins, menopause and neurodegeneration: basic and clinical studies. *Cell Mol Life Sci*. 2005;62(3):271—280.
8. Xu Y, López M. Central regulation of energy metabolism by estrogens. *Mol Metab*. 2018;15:104—115.
9. Osterlund MK, Grandien K, Keller E, Hurd YL. The human brain has distinct regional expression patterns of estrogen receptor alpha mRNA isoforms derived from alternative promoters. *J Neurochem*. 2000;75(4):1390—1397.
10. Osterlund MK, Gustafsson JA, Keller E, Hurd YL. Estrogen receptor beta (ERbeta) messenger ribonucleic acid (mRNA) expression within the human forebrain: distinct distribution pattern to ERalpha mRNA. *J Clin Endocrinol Metab*. 2000;85(10):3840—3846.
11. Irwin RW, Yao J, To J, Hamilton RT, Cadenas E, Brinton RD. Selective oestrogen receptor modulators differentially potentiate brain mitochondrial function. *J Neuroendocrinol*. 2012;24(1):236—248.
12. Yager JD, Chen JQ. Mitochondrial estrogen receptors—new insights into specific functions. *Trends Endocrinol Metabol*. 2007;18(3):89—91.
13. Sarkar S, Jun S, Simpkins JW. Estrogen amelioration of Aβ-induced defects in mitochondria is mediated by mitochondrial signaling pathway involving ERβ, AKAP and Drp1. *Brain Res*. 2015;1616:101—111.
14. Winer JR, Maass A, Pressman P, et al. Associations between tau, β-amyloid, and cognition in Parkinson disease. *JAMA Neurol*. 2018;75(2):227—235.
15. Minoshima S, Giordani B, Berent S, Frey KA, Foster NL, Kuhl DE. Metabolic reduction in the posterior cingulate cortex in very early Alzheimer's disease. *Ann Neurol*. 1997;42(1):85—94.
16. Small GW, Mazziotta JC, Collins MT, et al. Apolipoprotein E type 4 allele and cerebral glucose metabolism in relatives at risk for familial Alzheimer disease. *J Am Med Assoc*. 1995;273(12):942—947.

17. Simpson IA, Carruthers A, Vannucci SJ. Supply and demand in cerebral energy metabolism: the role of nutrient transporters. *J Cerebr Blood Flow Metabol*. 2007;27(11):1766—1791.
18. Sonntag WE, Ramsey M, Carter CS. Growth hormone and insulin-like growth factor-1 (IGF-1) and their influence on cognitive aging. *Ageing Res Rev*. 2005;4(2):195—212.
19. Annenkov A. The insulin-like growth factor (IGF) receptor type 1 (IGF1R) as an essential component of the signalling network regulating neurogenesis. *Mol Neurobiol*. 2009;40(3):195—215.
20. Rojanathammanee L, Rakoczy S, Kopchick J, Brown-Borg HM. Effects of insulin-like growth factor 1 on glutathione S-transferases and thioredoxin in growth hormone receptor knockout mice. *Age (Dordr)*. 2014;36(4):9687.
21. Gazit N, Vertkin I, Shapira I, et al. IGF-1 receptor differentially regulates spontaneous and evoked transmission via mitochondria at hippocampal synapses. *Neuron*. 2016;89(3):583—597.
22. Deng W, Aimone JB, Gage FH. New neurons and new memories: how does adult hippocampal neurogenesis affect learning and memory? *Nat Rev Neurosci*. 2010;11(5):339—350.
23. Mosconi L, Brys M, Switalski R, et al. Maternal family history of Alzheimer's disease predisposes to reduced brain glucose metabolism. *Proc Natl Acad Sci U S A*. 2007;104(48):19067—19072.
24. Brinton RD. The healthy cell bias of estrogen action: mitochondrial bioenergetics and neurological implications. *Trends Neurosci*. 2008;31(10):529—537.
25. Lane CA, Hardy J, Schott JM. Alzheimer's disease. *Eur J Neurol*. 2018;25(1):59—70.
26. Pike CJ. Sex and the development of Alzheimer's disease. *J Neurosci Res*. 2017;95(1—2):671—680.
27. Ryan J, Scali J, Carrière I, et al. Impact of a premature menopause on cognitive function in later life. *BJOG*. 2014;121(13):1729—1739.
28. Laws KR, Irvine K, Gale TM. Sex differences in cognitive impairment in Alzheimer's disease. *World J Psychiatr*. 2016;6(1):54—65.
29. Merlo S, Spampinato SF, Sortino MA. Estrogen and Alzheimer's disease: still an attractive topic despite disappointment from early clinical results. *Eur J Pharmacol*. 2017;817:51—58.
30. Engler-Chiurazzi EB, Brown CM, Povroznik JM, Simpkins JW. Estrogens as neuroprotectants: estrogenic actions in the context of cognitive aging and brain injury. *Prog Neurobiol*. 2017;157:188—211.
31. Engler-Chiurazzi EB, Singh M, Simpkins JW. Reprint of: from the 90's to now: a brief historical perspective on more than two decades of estrogen neuroprotection. *Brain Res*. 2016;1645:79—82.
32. Wang JM, Hou X, Adeosun S, et al. A dominant negative ERβ splice variant determines the effectiveness of early or late estrogen therapy after ovariectomy in rats. *PLoS One*. 2012;7(3):e33493.
33. López-Grueso R, Gambini J, Abdelaziz KM, et al. Early, but not late onset estrogen replacement therapy prevents oxidative stress and metabolic alterations caused by ovariectomy. *Antioxidants Redox Signal*. 2014;20(2):236—246.
34. Yao J, Irwin R, Chen S, Hamilton R, Cadenas E, Brinton RD. Ovarian hormone loss induces bioenergetic deficits and mitochondrial β-amyloid. *Neurobiol Aging*. 2012;33(8):1507—1521.
35. Lu Y, Sareddy GR, Wang J, et al. Neuron-Derived estrogen regulates synaptic plasticity and memory. *J Neurosci*. 2019;39(15):2792—2809.
36. Galluzzi L, Bravo-San Pedro JM, Kepp O, Kroemer G. Regulated cell death and adaptive stress responses. *Cell Mol Life Sci*. 2016;73(11—12):2405—2410.
37. Takasugi N, Tomita T, Hayashi I, et al. The role of presenilin cofactors in the gamma-secretase complex. *Nature*. 2003;422(6930):438—441.
38. Weksler ME, Szabo P, Relkin NR, Reidenberg MM, Weksler BB, Coppus AM. Alzheimer's disease and Down's syndrome: treating two paths to dementia. *Autoimmun Rev*. 2013;12(6):670—673.
39. Zhao Y, Bhattacharjee S, Jones BM, et al. Beta-amyloid precursor protein (βAPP) processing in Alzheimer's disease (AD) and age-related macular degeneration (AMD). *Mol Neurobiol*. 2015;52(1):533—544.
40. Yao Q, Feng M, Yang B, et al. Effects of ovarian hormone loss on neuritic plaques and autophagic flux in the brains of adult female APP/PS1 double-transgenic mice. *Acta Biochim Biophys Sin (Shanghai)*. 2018;50(5):447—455.
41. Yu W, Lu B. Synapses and dendritic spines as pathogenic targets in Alzheimer's disease. *Neural Plast*. 2012;2012:247150.
42. van Wijk N, Broersen LM, de Wilde MC, et al. Targeting synaptic dysfunction in Alzheimer's disease by administering a specific nutrient combination. *J Alzheimers Dis*. 2014;38(3):459—479.
43. Selkoe DJ, Hardy J. The amyloid hypothesis of Alzheimer's disease at 25 years. *EMBO Mol Med*. 2016;8(6):595—608.
44. Mosconi L, Brys M, Switalski R, et al. Maternal family history of Alzheimer's disease predisposes to reduced brain glucose metabolism. *Proc Natl Acad Sci U S A*. 2007;104(48):19067—19072.
45. Brinton RD. The healthy cell bias of estrogen action: mitochondrial bioenergetics and neurological implications. *Trends Neurosci*. 2008;31(10):529—537.
46. Magistretti PJ. Neuron-glia metabolic coupling and plasticity. *Exp Physiol*. 2011;96(4):407—410.
47. Wallace DC. A mitochondrial paradigm of metabolic and degenerative diseases, aging, and cancer: a dawn for evolutionary medicine. *Annu Rev Genet*. 2005;39:359—407.
48. Li PA, Hou X, Hao S. Mitochondrial biogenesis in neurodegeneration. *J Neurosci Res*. 2017;95(10):2025—2029.
49. Mosconi L, Mistur R, Switalski R, et al. Declining brain glucose metabolism in normal individuals with a maternal history of Alzheimer disease. *Neurology*. 2009;72(6):513—520.
50. Shi Y, Yamada K, Liddelow SA, et al. ApoE4 markedly exacerbates tau-mediated neurodegeneration in a mouse model of tauopathy. *Nature*. 2017;549(7673):523—527.
51. Wang Y, Mishra A, Brinton RD. Transitions in metabolic and immune systems from pre-menopause to post-menopause: implications for age-associated neurodegenerative diseases. *F1000Res*. 2020;9:F1000 Faculty Rev-68.
52. Duelli R, Kuschinsky W. Brain glucose transporters: relationship to local energy demand. *News Physiol Sci*. 2001;16:71—76.
53. Ding F, Yao J, Zhao L, Mao Z, Chen S, Brinton RD. Ovariectomy induces a shift in fuel availability and metabolism in the hippocampus of the female transgenic model of familial Alzheimer's. *PLoS One*. 2013;8(3):e59825.
54. Shi J, Simpkins JW. 17 beta-Estradiol modulation of glucose transporter 1 expression in blood-brain barrier. *Am J Physiol*. 1997;272(6 Pt 1):E1016—E1022.
55. Long J, He P, Shen Y, Li R. New evidence of mitochondria dysfunction in the female Alzheimer's disease brain: deficiency of estrogen receptor-β. *J Alzheimers Dis*. 2012;30(3):545—558.
56. Santagati S, Melcangi RC, Celotti F, Martini L, Maggi A. Estrogen receptor is expressed in different types of glial cells in culture. *J Neurochem*. 1994;63(6):2058—2064.
57. Frater J, Lie D, Bartlett P, McGrath JJ. Insulin-like Growth Factor 1 (IGF-1) as a marker of cognitive decline in normal ageing: a review. *Ageing Res Rev*. 2018;42:14—27.
58. Hoshi M, Sato M, Kondo S, et al. Different localization of tau protein kinase I/glycogen synthase kinase-3 beta from glycogen synthase kinase-3 alpha in cerebellum mitochondria. *J Biochem*. 1995;118(4):683—685.
59. Bijur GN, Jope RS. Glycogen synthase kinase-3 beta is highly activated in nuclei and mitochondria. *Neuroreport*. 2003;14(18):2415—2419.
60. Yang K, Chen Z, Gao J, et al. The key roles of GSK-3β in regulating mitochondrial activity. *Cell Physiol Biochem*. 2017;44(4):1445—1459.
61. Hoeflich KP, Luo J, Rubie EA, Tsao MS, Jin O, Woodgett JR. Requirement for glycogen synthase kinase-3beta in cell survival and NF-kappaB activation. *Nature*. 2000;406(6791):86—90.